

FIR FILTERS COMPLIANT WITH THE IEEE STANDARD FOR M CLASS PMU

Krzysztof Duda¹⁾, Tomasz P. Zieliński²⁾

1) AGH University of Science and Technology, Faculty of Electrical Engineering, Automatics, Computer Science and Biomedical Engineering, Al. A. Mickiewicza 30, 30-059 Kraków, Poland (✉ kduda@agh.edu.pl, +48 12 617 2841)

2) AGH University of Science and Technology, Faculty of Computer Science, Electronics and Telecommunications, Al. A. Mickiewicza 30, Kraków, Poland (tzielin@agh.edu.pl)

Abstract

In this paper it is shown that M class PMU (*Phasor Measurement Unit*) reference model for phasor estimation recommended by the IEEE Standard C37.118.1 with the Amendment 1 is not compliant with the Standard. The reference filter preserves only the limits for TVE (*total vector error*), and exceeds FE (*frequency error*) and RFE (rate of frequency error) limits. As a remedy we propose new filters for phasor estimation for M class PMU that are fully compliant with the Standard requirements. The proposed filters are designed: 1) by the window method; 2) as flat-top windows; or as 3) optimal min-max filters. The results for all Standard compliance tests are presented, confirming good performance of the proposed filters. The proposed filters are fixed at the nominal frequency, *i.e.* frequency tracking and adaptive filter tuning are not required, therefore they are well suited for application in low-cost popular PMUs.

Keywords: phasor estimation, phasor measurement unit, FIR filter, cosine window, flat-top window.

© 2016 Polish Academy of Sciences. All rights reserved

1. Introduction

A phasor as defined by the Standard [1] plays significant role in the electric power system management [3, 4]. *Phasor Measurement Units* (PMUs) are designed for measuring synchrophasors, *i.e.* phasors with reference to the standard time. The problem of phasor estimation is addressed in many writings, *e.g.* [5–24]. The Standard compliance tests [1, 2] may be used for comparing and evaluating phasor estimation algorithms. Such comparisons may also include additional criteria not covered in the Standard, *e.g.* computational complexity. In general, the accuracy of phasor estimation algorithms may be improved at the cost of increased processing delay and increased computational complexity. Phasor estimation algorithms are often based on DFT (*Discrete Fourier Transform*) or IpDFT (*Interpolated DFT*) [5–12]. An extension of the DFT analysis is the Taylor–Fourier transform [13–15]. The DFT and the Taylor–Fourier transform may be applied as band-pass complex-coefficient FIR (*Finite Impulse Response*) filters. The phasor may also be estimated by a *low-pass* (LP) FIR filtering after signal demodulation with a quadrature oscillator [18–24], as recommended by the Standard [1, Fig. C.1]. The quadrature oscillator may either be fixed at the nominal frequency or tuned to an actual frequency with the benefit of higher estimation accuracy. The standard reference LP FIR filter is fixed at the nominal frequency [1]. It is only compliant with TVE (*total vector error*), and does not preserve the limits for FE (*frequency error*) and RFE (*rate of frequency error*).

The contribution of this paper is a design of LP FIR filters fixed at the nominal frequency and preserving the limits for TVE, FE, and RFE in all compliance tests of the Standard [1, 2]. The new fully compliant filters are designed: 1) by the window method [25]; 2) as the perfectly *flat-top* (FT) windows [26]; or as 3) the optimal min-max filters [27]. The window method of designing LP FIR filters for phasor estimation is recommended by the Standard [1, 2], although

the parameters of fully compliant filters are not given there. The application of FT windows as LP FIR filters for phasor estimation is a new concept, which is an important contribution of this paper. These new filters very accurately estimate the frequency and its rate of change. The optimal min-max filters were found by simultaneous minimization of TVE, FE and RFE errors in all compliance tests. For the above three families of FIR filters ready to use designs are given and compared in this paper. It is shown that all of them are fully compliant with the IEEE Standard C37.118.1 requirements.

2. Signal model and phasor definition

Consider a continuous-time narrow-band sinusoidal signal:

$$x(t) = a(t) \cos(\omega_0 t + \varphi(t)), \quad (1)$$

where: $\omega_0 = 2\pi f_0$ is a nominal pulsation in rad/s; f_0 is a nominal frequency in Hz; $a(t)$ is a time-varying amplitude; and $\varphi(t)$ is a time-varying phase in radians. The phasor of (1), in respect to the frequency f_0 , is defined as:

$$p(t) = \frac{a(t)}{\sqrt{2}} e^{j\varphi(t)}. \quad (2)$$

The equations (1) and (2) are related by:

$$x(t) = \text{Re} \{ \sqrt{2} p(t) e^{j\omega_0 t} \}. \quad (3)$$

The phasor reporting rates F_{RR} are given in [1, Table 1] for 50 Hz and 60 Hz systems. For the $f_0 = 50$ Hz nominal frequency system the phasor should be estimated 10, 25, or 50 times per second. In this paper fully compliant FIR filters for $f_0 = 50$ Hz and $F_{RR} = 50$ Hz for the M class PMU are designed, and examples of filters compliant for $F_{RR} = \{10, 25\}$ Hz are given.

The instantaneous frequency f_{in} of (1) is the 1st order time derivative of the cosine argument in (1) [1]:

$$f_{in}(t) = f_0 + \frac{1}{2\pi} \frac{d\varphi(t)}{dt}, \quad (4)$$

and the *rate of change of frequency* (ROCOF) is the 2nd order time derivative of the cosine angle [1]:

$$ROCOF(t) = \frac{1}{2\pi} \frac{d^2\varphi(t)}{d^2t} = \frac{df_{in}(t)}{dt}. \quad (5)$$

If $f_{in} \neq f_0$, the phasor rotates on the complex plain. For example, the values of phasors for $f_{in} = 50$ Hz and $f_{in} = 51$ Hz for the $f_0 = 50$ Hz system and for $f_{in} = 60$ Hz and $f_{in} = 61$ Hz for the $f_0 = 60$ Hz system are given in [1, Table 2] for the 10 Hz reporting rate.

The digital signal $x[n]$ corresponding to (1) is obtained by anti-aliasing analog LP filtering and sampling by an analog-to-digital converter:

$$x[n] = a[n] \cos(\Omega_0 n + \varphi[n]), \quad \Omega_0 = 2\pi \frac{f_0}{f_s}, \quad (6)$$

where Ω_0 is a normalized frequency (pulsation) in radians of the discrete-time signal, and $n = -N, \dots, 0, \dots, N$ is the sample index. In the Standard the values of digital complex phasor are found by multiplying $x[n]$ with the quadrature oscillator (frequency converter to DC) and extraction of a near-DC component by LP FIR filtering [1, Fig. C.1]. The LP filter limits the spectrum of the phasor $p[n]$ below half of the reporting rate F_{RR} . In the passband the filter should be flat from 0 to 5 Hz to ensure accurate amplitude estimation.

The instantaneous frequency of signal (1) is estimated as [2]:

$$f_{in}[n] = f_0 + \frac{f_s}{2\pi} \frac{\varphi[n+1] - \varphi[n-1]}{2}, \quad (7)$$

and the rate of change of frequency is estimated as [2]:

$$ROCOF[n] = \frac{f_s^2}{2\pi} \frac{\varphi[n+2] - 2\varphi[n] + \varphi[n-2]}{4}. \quad (8)$$

3. Low-pass FIR filters for phasor estimation

3.1. Standard reference FIR filter

The coefficients of the standard reference LP FIR filter designed by the window method [25] are defined as [1, 2]:

$$h_{LP}[n] = \begin{cases} \frac{\sin(A)}{A} h[n], & A = 2\pi \frac{2f_{fr}}{f_s} n, \quad n = -N, \dots, N - \{0\} \\ 1, & n = 0 \end{cases}. \quad (9)$$

where f_{fr} denotes the filter reference frequency [1, 2], which is equal to half of the filter cut-off frequency [25], and $h[n]$ is the Hamming window of length $L = 2N + 1$. The DC gain of the standard filter (9) is equal to 1 if $h[n]$ is divided by the sum of all coefficients. The values of f_{fr} and N for different nominal frequencies (50 or 60 Hz) and different reporting rates F_{RR} are given in [2, Table C.1]. In Section 4 it is shown that the Standard reference model meets the Standard limits only for the TVE error.

Fully compliant FIR filters can be designed by the window method. The compliant filters are obtained by proper selection of a window type, its length, and the reference frequency f_{fr} . The maximum length of the filter is limited by the allowed reporting latency [1, 2]. We have found that fully compliant filters may be obtained using the Hann window, the Blackman window, and the Rife-Vincent class I order 2 window (known also as the maximum side-lobe decay window or $\sin^\alpha(x)$ $\alpha = 4$ window [28]). However, we were unable to obtain a fully compliant filter with the Hamming window recommended by the Standard [1, 2].

3.2. New flat-top FIR filters

Flat-top (FT) windows have a unique feature of the spectral main lobe being perfectly flat or equiripple and – simultaneously – fast decaying of the sidelobes. The FT windows are cosine windows defined as [26]:

$$h_M[n] = w_M[n] = \begin{cases} \sum_{m=0}^M a_M[m] \cos(m \frac{\pi}{N} n), & n = -N, \dots, N \\ 0, & \text{otherwise} \end{cases}. \quad (10)$$

where M is the window order and $a_M[m]$ are the coefficients of an M -order window. The window (10) has $L = 2N + 1$ samples. The discrete-time sequence (10) may be used for signal windowing carried out by multiplication or for signal filtering carried out by discrete convolution. In this work we consider an FT window as an LP filter, which is denoted by $h_M[n] = w_M[n]$. By increasing M the passband width increases, and the passband flatness and the stopband attenuation may be improved. For a given M the cut-off frequency of the filter $h_M[n]$ can be adjusted by the length of its impulse response L . In [26] the coefficients $a_M[m]$ of 13 new perfectly flat and equiripple FT windows were proposed. Computer simulations showed that both perfectly flat and equiripple FT windows may be used for obtaining fully compliant

M class PMU filters. However, for a given order M the performance of perfectly flat and equiripple FT windows is similar. For that reason only the results for perfectly flat windows are presented next. The designing of perfectly flat-top filters is explained in Appendix A.

3.3. Optimal min-max filters

Min-max LP filters are optimal Chebyshev approximations and have an equiripple magnitude response in the passband and in the stopband [27]. Designing min-max filters is based on the Remez exchange algorithm and is implemented, e.g., in the Matlab Signal Processing Toolbox [27] as the function *firpm* (where PM denotes the Parks-McClellan algorithm). The LP filter design requires 5 parameters: the length L of the filter, the passband and stopband edge frequencies f_{pass} and f_{stop} , and the weights in the passband and the stopband w_{pass} and w_{stop} , respectively. For fully compliant filters those parameters are determined by simultaneous minimization of TVE, FE and RFE errors in all compliance tests. We have found that fully compliant filters are obtained for $f_{pass} = 4.6$ Hz, $w_{pass} = 1$, and $w_{stop} = 1400$, and the following stopband frequencies depending on the filter length: $L = 197$ and $f_{stop} = 25.7$ Hz, $L = 199$ and $f_{stop} = 25.6$ Hz, $L = 201$ and $f_{stop} = 25.6$ Hz, $L = 203$ and $f_{stop} = 25.5$ Hz, $L = 205$ and $f_{stop} = 25.5$ Hz, $L = 207$ and $f_{stop} = 25.4$ Hz, $L = 209$ and $f_{stop} = 25.3$ Hz, $L = 211$ and $f_{stop} = 25.3$ Hz, $L = 213$ and $f_{stop} = 25.2$ Hz, $L = 215$ and $f_{stop} = 25.2$ Hz, $L = 217$ and $f_{stop} = 25.1$ Hz, $L = 219$ and $f_{stop} = 25.1$ Hz.

4. Results

4.1. Magnitude responses

The Standard [1, 2] defines the M (measurement) class reference model for phasor estimation for the $f_0 = 60$ Hz nominal frequency. The sampling frequency is $f_s = 960$ Hz, *i.e.* 16 samples per one cycle of nominal frequency are taken. For the $f_0 = 50$ Hz system the same number of samples per one cycle is obtained with the sampling frequency $f_s = 800$ Hz. The length of the reference filter for the $f_0 = 50$ Hz system for $f_s = 800$ Hz and $F_{RR} = 50$ Hz is $L = 143$ samples. The impulse response of the reference filter is depicted in Figure 1, and its magnitude response is shown in Fig. 2. Figs. 1 and 2 also present fully compliant FIR filters designed:

- 1) by the window method (9) with the Blackman window ($L = 197$, $f_{fr} = 6.65$ Hz), the Hann window ($L = 199$, $f_{fr} = 5.75$ Hz), and the Rife-Vincent class I order 2 (RV2) window ($L = 213$, $f_{fr} = 6.7$ Hz);
- 2) as flat-top windows (10) (FT, $M = 4$: $L = 199$, $D_0 = 2$, $D_N = 1$, FT, $M = 5$: $L = 207$, $D_0 = 2$, $D_N = 2$);
- 3) as a min-max optimal LP filter (denoted by optimal FIR) with parameters $L = 197$, $f_{pass} = 4.6$ Hz, $f_{stop} = 25.7$ Hz, $w_{pass} = 1$, and $w_{stop} = 1400$.

The FIR filter delay must not exceed the allowed reporting latency, which equals to 7 reporting times, *i.e.* $7/F_{RR}$, for the M class PMU [2, Table 11]. Therefore, the FIR filter impulse response must not exceed 14 reporting times. The maximum allowed filter length for the $f_s = 800$ Hz and $F_{RR} = 50$ Hz system is equal to 224 samples. It is also convenient to use filters with an odd length and symmetrical impulse response in the middle sample.

While searching for a fully compliant *flat-top* (FT) FIR filters we have tested all 49 FT windows reported in [26] and some other FT windows designed by the procedure given in [26], with the length L changing from 79 samples to 223 samples. From this broad set only 4 windows have passed all tests of the Standard.

The compliant windows are:

- 1) FT, $M = 4$, $D_0 = 2$, $D_N = 1$, $L = 199$;

- 2) FT, $M = 4$, $D_0 = 0$, $D_N = 1$, $\delta = [0 \ 0.339463745 \ 0.481494823]$, $L = 201$;
- 3) FT, $M = 5$, $D_0 = 0$, $D_N = 2$, $\delta = [0 \ 0.3396586 \ 0.481532356]$, $L = 207$;
- 4) FT, $M = 5$, $D_0 = 2$, $D_N = 2$, $L = 207$.

Where the meaning of the symbols D_0 , D_N , δ is the same as in [26]. The length L given in the above list of four fully compliant windows is the shortest possible length. A window may also be compliant for higher values of L , e.g. the window #1 is compliant for all odd lengths in the closed interval from 199 to 215. The window #4 was not given in [26]. The windows #1 and #2, and the windows #3 and #4 give similar results in compliance tests. For that reason further results are presented only for perfectly flat-top windows #1 and #4. Fig. 1 shows the impulse responses of the FT compliant filters, whereas Fig. 2 depicts their magnitude responses. In Fig. 2 fast decaying of the sidelobes and the flat passband are observed for the FT filters. The coefficients of the FT filters are given in Table 1.

For different sampling frequencies the proposed FT FIR filters comply all standard tests, if the length of their impulse response equals to approximately 13 periods of the nominal frequency.

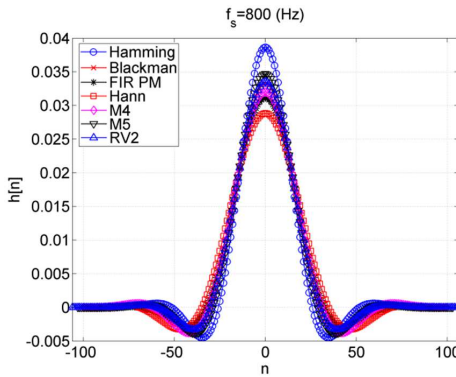


Fig. 1. The impulse responses of phasor estimation FIR filters normalized for DC gain equal to 1. The filters' parameters are: Hamming: $L=143$, $f_{fr}=7.75$ Hz; Blackman: $L=197$, $f_{fr}=6.65$ Hz; optimal FIR: $L=197$, $f_{pass}=4.6$ Hz, $f_{stop}=25.7$ Hz, $w_{pass}=1$, $w_{stop}=1400$; Hann: $L=199$, $f_{fr}=5.75$ Hz; FT, $M=4$: $D_0=2$, $D_N=1$, $L=199$; FT, $M=5$: $D_0=2$, $D_N=2$, $L=207$; RV2: $L=213$, $f_{fr}=6.7$ Hz.

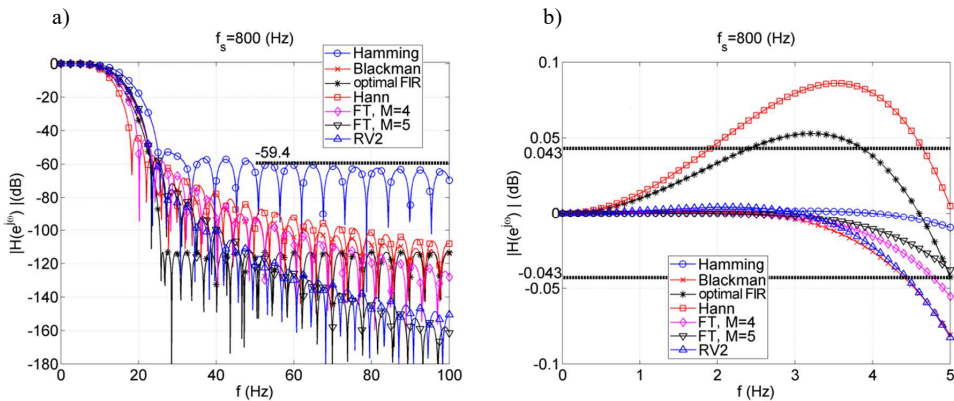


Fig. 2. The magnitude responses of phasor estimation FIR filters. The filters' parameters are the same as in Fig. 1. a) The Standard recommendation for frequencies above 50 Hz is -59.4 dB [2, Fig. C.5]. b) The Standard recommendation for frequencies from 0 to 5 Hz is 0 ± 0.043 dB [2, Fig. C.5].

For given f_s and F_{RR} the length of the proposed FT FIR filter compliant with the Standard is:

$$L \approx 13 \frac{f_s}{F_{RR}}. \tag{11}$$

The exact number of samples is established by computer simulations. As an example Table 2 gives $M = 4, D_0 = 2, D_N = 1$ FT window coefficients for compliant FIR filters for the sampling frequencies $f_s = 400$ Hz and $f_s = 1600$ Hz, and the reporting rate $F_{RR} = 50$ Hz.

It is observed in Fig. 2 that all filters meet the Standard recommendation [2, Fig. C.5] in the stopband and the proposed filters do this in excess. Surprisingly, as seen in Fig. 2b, only the reference filter and the FT, $M = 5$ filter meet the Standard recommendation in the passband. The remaining filters do not fit into the Standard recommendation in the passband, yet, as shown next, they are all fully compliant.

Table 1. The coefficients of compliant new flat-top PMU filters for the sampling frequency $f_s = 800$ Hz.

$M = 4, D_0 = 2, D_N = 1, L = 199$ 12.4375 cycles of f_0	$M = 5, D_0 = 2, D_N = 2, L = 207$ 12.9375 cycles of f_0
$a_4[0] = 1.005050505051$	$a_5[0] = 1.004854368932$
$a_4[1] = 2.006242473998$	$a_5[1] = 2.007611297343$
$a_4[2] = 1.853902546302$	$a_5[2] = 1.917918999420$
$a_4[3] = 1.176285932351$	$a_5[3] = 1.451047039136$
$a_4[4] = 0.323575354997$	$a_5[4] = 0.666862839032$
	$a_5[5] = 0.130977870905$

Table 2. The coefficients of a compliant flat-top PMU filter $M = 4, D_0 = 2, D_N = 1$ for different sampling frequencies.

$f_s = 400$ Hz, $L = 101$ 12.625 cycles of f_0	$f_s = 1600$ Hz, $L = 405$ 12.65625 cycles of f_0
$a_4[0] = 1.010000000000$	$a_4[0] = 1.002475247525$
$a_4[1] = 2.016122461957$	$a_4[1] = 2.001101845739$
$a_4[2] = 1.863032315327$	$a_4[2] = 1.849152261195$
$a_4[3] = 1.182078693510$	$a_4[3] = 1.173271915521$
$a_4[4] = 0.325168840140$	$a_4[4] = 0.322746252540$

4.2. Compliance tests

Table 3 presents normalized compliance test errors of phasor estimation obtained for the $f_s = 800$ Hz and $F_{RR} = 50$ Hz PMU system for filters presented in Figs. 1 and 2. The columns are ordered according to the increasing value of filter length L . The signal duration in every test was 10 s, and the test signal parameters were set as recommended by the Standard [1, 2]. Table 3 shows the TVE [1, (12)], the FE [1, (13)], and the RFE [1, (14)] values for all tests from the Standard [1, 2] in consecutive rows. The number in brackets gives the filter position in the test (ascending sort along rows).

For easier inspection all errors in Table 3 are divided by the required standard limits, what means that the value lower than 1 confirms compliance with the Standard. From Table 3 it is seen that only the reference standard filter with the Hamming window $L = 143$, and $f_{fr} = 7.75$ Hz does not preserve all errors limits. The reference filter keeps only the limits of TVE, but exceeds FE and RFE limits (bolded values in Table 3). The flat-top filter is the most frequent winner.

It is observed in Table 3 that the proposed FT filters pass the out-of-band interference test [1, 2] but give the results close to the limits. The maximum TVE and FE errors along with the Standard limits for this test are shown in Fig. 3 for all filters. The standard reference filter fails to pass this test in the frequency measurement.

Table 3. The normalized compliance test errors for different filters. Sampling frequency $f_s = 800$ Hz and reporting rate $F_{RR} = 50$ Hz.

Standard test	Hamming $f_{fr} = 7.75$ Hz $L = 143$	Blackman $f_{fr} = 6.65$ Hz $L = 197$	Optimal FIR $f_{stop} = 25.7$ Hz $L = 197$	Hann $f_{fr} = 5.75$ Hz $L = 199$	FT, $M = 4$, $D_0 = 2, D_N = 1$, $L = 199$	FT, $M = 5$, $D_0 = 2, D_N = 2$, $L = 207$	RV2 $f_{fr} = 6.7$ Hz $L = 213$
S1, TVE	1.5e-001 (1)	9.3e-001 (5)	6.0e-001 (3)	0.9954 (7)	6.4e-001 (4)	4.4e-001 (2)	9.5e-001 (6)
S2, TVE	2.5e-002 (7)	4.4e-004 (5)	2.0e-004 (3)	5.0e-004 (6)	2.4e-004 (4)	7.1e-006 (2)	6.1e-006 (1)
S3, TVE	3.9e-002 (7)	2.2e-004 (5)	2.2e-004 (4)	4.3e-004 (6)	4.3e-005 (3)	9.2e-007 (1)	3.3e-006 (2)
S4, TVE	3.2e-001 (5)	3.1e-002 (1)	4.2e-001 (6)	5.9e-001 (7)	4.0e-002 (3)	3.4e-002 (2)	6.2e-002 (4)
S5, TVE	4.6e-002 (7)	1.4e-003 (2)	5.3e-004 (1)	7.3e-003 (4)	9.6e-003 (5)	1.0e-002 (6)	6.4e-003 (3)
S6, TVE	3.1e-001 (5)	3.1e-002 (1)	4.2e-001 (6)	5.9e-001 (7)	4.0e-002 (3)	3.4e-002 (2)	6.2e-002 (4)
S1, FE	11.36 (7)	4.1e-002 (5)	4.1e-002 (4)	7.6e-002 (6)	1.2e-002 (3)	2.8e-004 (1)	6.2e-004 (2)
S2, FE	1.18 (7)	2.9e-003 (4)	8.0e-003 (5)	1.2e-002 (6)	2.5e-003 (3)	1.8e-004 (1)	2.8e-004 (2)
S3, FE	1.20 (7)	6.5e-003 (5)	6.0e-003 (4)	1.2e-002 (6)	1.3e-003 (3)	2.7e-005 (1)	9.6e-005 (2)
S4, FE	13.92 (7)	9.2e-001 (4)	6.0e-001 (2)	4.7e-001 (1)	9.9e-001 (6)	8.9e-001 (3)	9.7e-001 (5)
S5, FE	4.05 (7)	6.8e-002 (2)	3.2e-002 (1)	2.6e-001 (4)	3.2e-001 (5)	3.2e-001 (6)	2.1e-001 (3)
S6, FE	13.33 (7)	9.3e-001 (4)	6.0e-001 (2)	4.8e-001 (1)	9.9e-001 (6)	8.9e-001 (3)	9.7e-001 (5)
D1, TVE	1.3e-002 (1)	3.4e-002 (5)	2.2e-002 (3)	3.7e-002 (7)	2.4e-002 (4)	1.6e-002 (2)	3.5e-002 (6)
D2, TVE	1.7e-002 (1)	3.4e-002 (5)	2.7e-002 (4)	3.4e-002 (6)	2.6e-002 (3)	1.8e-002 (2)	3.5e-002 (7)
D3, TVE	1.3e-001 (1)	8.1e-001 (5)	6.1e-001 (4)	0.9967 (7)	5.4e-001 (3)	3.7e-001 (2)	8.2e-001 (6)
D4, TVE	1.3e-001 (1)	8.1e-001 (5)	6.1e-001 (4)	0.9967 (7)	5.4e-001 (3)	3.7e-001 (2)	8.2e-001 (6)
D1, FE	1.2e-001 (7)	7.4e-004 (4)	7.8e-004 (5)	1.4e-003 (6)	1.4e-004 (3)	3.1e-006 (1)	1.1e-005 (2)
D2, FE	1.1e-001 (7)	1.6e-002 (6)	9.3e-003 (2)	1.3e-002 (4)	1.1e-002 (3)	7.8e-003 (1)	1.6e-002 (5)
D3, FE	5.70 (7)	2.4e-002 (4)	2.6e-002 (5)	4.5e-002 (6)	1.0e-002 (3)	3.4e-003 (1)	3.7e-003 (2)
D4, FE	5.70 (7)	2.4e-002 (4)	2.6e-002 (5)	4.5e-002 (6)	1.0e-002 (3)	3.4e-003 (1)	3.7e-003 (2)
D1, RFE	2.0e-001 (7)	2.5e-004 (5)	1.8e-004 (4)	3.0e-004 (6)	1.5e-004 (3)	3.1e-006 (2)	1.6e-006 (1)
D2, RFE	2.4e-001 (7)	1.1e-002 (5)	6.8e-003 (3)	6.6e-003 (2)	7.3e-003 (4)	4.9e-003 (1)	1.1e-002 (6)
D3, RFE	171.19 (7)	5.4e-001 (4)	6.2e-001 (5)	9.9e-001 (6)	1.5e-001 (3)	3.6e-003 (1)	8.3e-003 (2)
D4, RFE	171.19 (7)	5.4e-001 (4)	6.2e-001 (5)	9.9e-001 (6)	1.5e-001 (3)	3.6e-003 (1)	8.3e-003 (2)
Max error	171.19 (7)	9.3e-001 (3)	6.2e-001 (1)	0.9967 (6)	9.9e-001 (5)	8.9e-001 (2)	9.7e-001 (4)
Mean Max error	16.70 (7)	2.4e-001 (5)	2.2e-001 (4)	3.2e-001 (6)	1.9e-001 (2)	1.4e-001 (1)	2.1e-001 (3)
Mean Mean error	16.30 (7)	2.1e-001 (4)	2.2e-001 (5)	3.2e-001 (6)	1.6e-001 (2)	1.2e-001 (1)	1.8e-001 (3)

Legend:

The failed tests have normalized errors above 1 and they are bolded.

The number in brackets gives the filter position in the test (ascending sort along rows).

The tests are [1, 2]:

S1: Static compliance $45 < f_{in} < 55$, TVE limit 1%, FE limit 0.005 Hz.

S2: Static compliance 10% of 2nd harmonic, TVE limit 1%, FE limit 0.025 Hz.

S3: Static compliance 10% of 3rd harmonic, TVE limit 1%, FE limit 0.025 Hz.

S4: Static compliance out-of-band interference (OfB), $f_{in} = 47.5$ Hz, TVE limit 1.3 %, FE limit 0.01 Hz.

S5: Static compliance out-of-band interference, $f_{in} = 50$ Hz, TVE limit 1.3 %, FE limit 0.01 Hz.

S6: Static compliance out-of-band interference, $f_{in} = 52.5$ Hz, TVE limit 1.3 %, FE limit 0.01 Hz.

D1: Dynamic compliance, amplitude modulation (AM) $k_x = 0.1, k_a = 0$, TVE limit 3%, FE limit 0.3 Hz, RFE limit 14 Hz/s.

D2: Dynamic compliance, phase modulation (PM) $k_x = 0, k_a = 0.1$, TVE limit 3%, FE limit 0.3 Hz, RFE limit 14 Hz/s.

D3: Dynamic compliance, positive ramp (linear frequency modulation LFM), TVE limit 1%, FE limit 0.01 Hz, RFE limit 0.2 Hz/s.

D4: Dynamic compliance, negative ramp, TVE limit 1%, FE limit 0.01 Hz, RFE limit 0.2 Hz/s.

The proposed FT filters are good in estimation of the instantaneous frequency (7) and its rate of change (8). As an example, TVE, FE and RFE errors in the frequency ramp tests are presented in Fig. 4. Fig. 4a shows that the TVE for the proposed FT filter is over 100 times smaller than for the standard filter in the wide range of signal instantaneous frequency. The FE

error of the proposed FT filters, Fig. 4b, is over 100 times smaller than the Standard limit. The RFE error, Fig. 4c, for the proposed $L = 207$ FT filter is also more than 100 times smaller than the Standard limit.

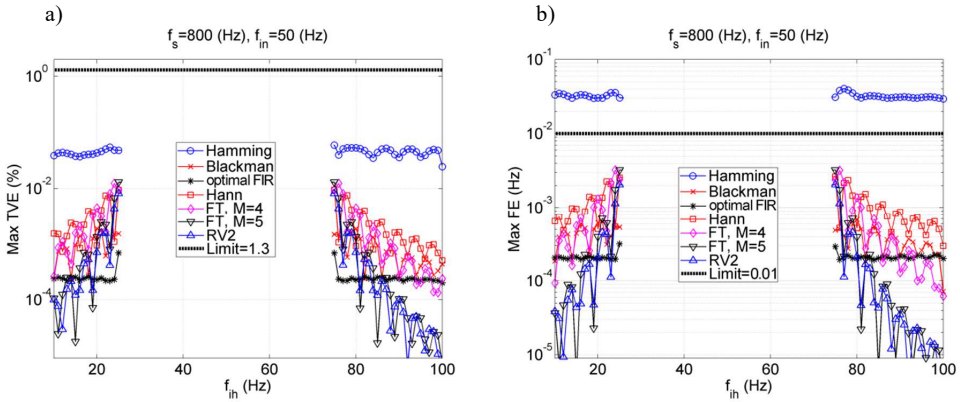


Fig. 3. The out-of-band interference test. The input test signal frequency $f_{in} = 50$ Hz, f_{ih} is the frequency of interfering signal; a) Maximum TVE error, b) Maximum FE error. The filters' parameters are the same as in Fig. 1.

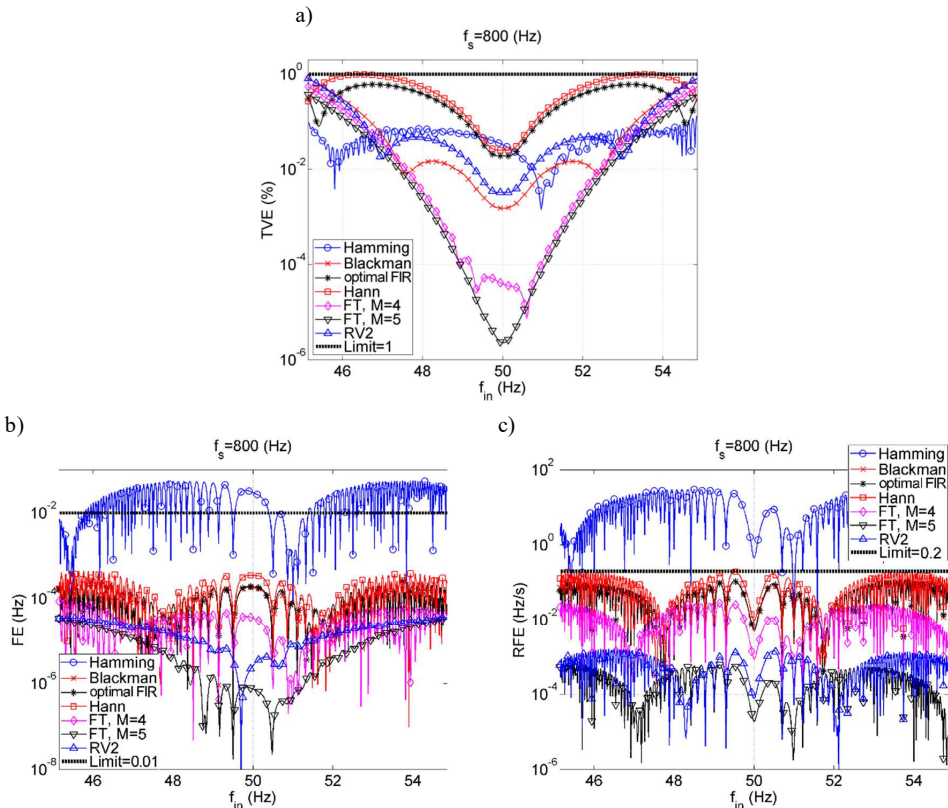


Fig. 4. The positive ramp of system frequency test. The input test signal frequency f_{in} changes linearly from 45 Hz to 55 Hz with the rate 1 Hz/s; a) TVE error, b) FE error, c) RFE error. The filters' parameters are the same as in Fig. 1.

Table 4. The maximum and mean errors from all compliance tests for different filter lengths L .

L	Filter	Max error	Mean Max error	Mean Mean error
143	Hamming, $f_r = 7.75$ Hz	171.19	16.70	16.30
197	Optimal FIR, $f_{stop} = 25.7$ Hz	0.6160	0.2204	0.2167
197	Blackman, $f_r = 6.65$ Hz	0.9276	0.2414	0.2145
199	Optimal FIR, $f_{stop} = 25.6$ Hz	0.5855	0.2069	0.2036
199	Blackman, $f_r = 6.65$ Hz	0.8571	0.2262	0.2011
199	FT, $M = 4, D_0 = 2, D_N = 1$	0.9937	0.1888	0.1647
199	Hann, $f_r = 5.75$ Hz	0.9967	0.3190	0.3214
207	Optimal FIR, $f_{stop} = 25.4$ Hz	0.4285	0.1524	0.1495
207	Blackman, $f_r = 6.7$ Hz	0.6083	0.1748	0.1575
207	FT, $M = 4, D_0 = 2, D_N = 1$	0.7909	0.1567	0.1375
207	FT, $M = 5, D_0 = 2, D_N = 2$	0.8905	0.1429	0.1225
207	Hann, $f_r = 5.5$ Hz	0.9794	0.3099	0.3123
211	Optimal FIR, $f_{stop} = 25.3$ Hz	0.3628	0.1278	0.1247
211	FT, $M = 5, D_0 = 2, D_N = 2$	0.4868	0.0996	0.0863
211	Blackman, $f_r = 6.65$ Hz	0.5619	0.1517	0.1369
211	FT, $M = 4, D_0 = 2, D_N = 1$	0.8788	0.1550	0.1361
211	Hann, $f_r = 5.35$ Hz	0.9446	0.3049	0.3062
213	Optimal FIR, $f_{stop} = 25.2$ Hz	0.3297	0.1164	0.1142
213	FT, $M = 5, D_0 = 2, D_N = 2$	0.5131	0.1005	0.0870
213	Blackman, $f_r = 6.75$ Hz	0.5346	0.1398	0.1270
213	FT, $M = 4, D_0 = 2, D_N = 1$	0.9255	0.1575	0.1383
213	Hann, $f_r = 5.3$ Hz	0.9452	0.3015	0.3036
213	RV2, $f_r = 6.7$ Hz	0.9724	0.2075	0.1791
219	Optimal FIR, $f_{stop} = 25.1$ Hz	0.2409	0.0838	0.0811
219	Blackman, $f_r = 6.8$ Hz	0.4196	0.1074	0.0980
219	FT, $M = 5, D_0 = 2, D_N = 2$	0.5989	0.1058	0.0917
219	RV2, $f_r = 6.7$ Hz	0.7071	0.1509	0.1317
219	Hann, $f_r = 7$ Hz	0.9233	0.2421	0.2308

The last three rows in Table 3 present overall errors from all compliance tests. These errors are defined for easy global comparison of filters.

Max error is the normalized maximum error from all tests. For the fully compliant filter the value must be lower than 1. *Mean Max error* is the mean value of maximum errors from all compliance tests. *Mean Mean error* is the mean value of mean errors from all compliance tests. This error is proportional to the area under the error function. The broad comparison of the filters in the sense of above three errors is presented in Table 4 for different filter lengths L . For a given length L the rows are sorted according to the increasing value of *Max error*. It is seen that the optimal filter is the best in the sense of *Max error*, and the smallest *Max error* obtained for $L = 219$ equals to 0.2409. The smallest *Mean Mean error* equalled to 0.0811 was also obtained by the optimal filter $L = 219$. The second smallest *Mean Mean error* equalled to 0.0863 was obtained by FT filter FT, $M = 5, D_0 = 2, D_N = 2, L = 211$.

4.3. Remaining reporting rates

The results similar to the presented above for the reporting rate $F_{RR} = 50$ Hz can also be obtained for the reporting rates $F_{RR} = 10$ Hz and $F_{RR} = 25$ Hz recommended by the Standard [1, Table 1]. The detailed analysis of filters' performance for $F_{RR} = 10$ Hz and $F_{RR} = 25$ Hz is not presented here. We only summarize that for $f_s = 800$ Hz, and $F_{RR} = 10$ Hz [2, Table C1] the flat-top equiripple filter with length $L = 1071$, order $M = 5$ and coefficients (10) $a_s[m] = [1.0009345794, 2.0004235406, 2.0023075241, 2.0012570792, 1.7499164689, 0.7514779527]$ is fully compliant with the Standard. *Max error* for this filter equals to 0.66. In

this case the standard filter has *Max error* equal to 41.63 and it is not compliant, it does not preserve even TVR errors in the ramp test (*i.e.* D3, and D4 in Table 3). For $f_s = 800$ Hz, and $F_{RR} = 25$ Hz [2, Table C1] fully compliant is the flat-top equiripple filter of length $L = 425$, order $M=5$ and with coefficients (10) $a_5[m] = [1.0023584906, 2.0062191835, 2.0049355827, 1.9296489327, 1.3178926474, 0.3893186044]$. *Max error* for this filter equals to 0.81. The standard filter in this case has *Max error* equalled to 87.22, and is not compliant. Fig. 5 presents the frequency responses of the proposed flat-top compliant filters for $f_s = 800$ Hz, and $F_{RR} = 10$ Hz and 25 Hz, in comparison with the standard filters that are not compliant.

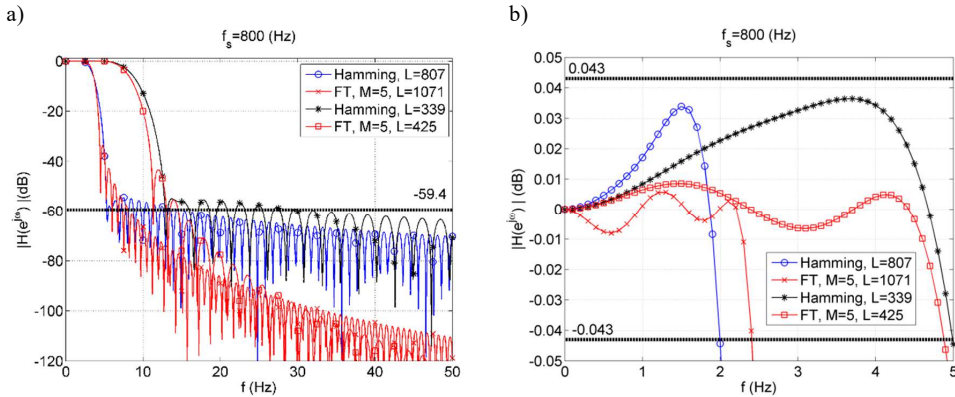


Fig. 5. The magnitude responses of phasor estimation FIR filters for $F_{RR} = 10$ Hz and $F_{RR} = 25$ Hz. FT, $M = 5$, $L = 1071$ denotes the filter compliant for $F_{RR} = 10$ Hz, and FT, $M = 5$, $L = 425$ denotes the filter compliant for $F_{RR} = 25$ Hz. For comparison the standard filters designed with Hamming window are shown [2, Table C1]. a) Stopband; b) Passband.

5. Conclusion

In this paper we have shown that the Standard [1, 2] specifies the reference model for PMU estimation that is not compliant with its own requirements. Also, we have proposed new compliant filters. The designing of a compliant filter is not a trivial task, nevertheless we have demonstrated in this work that even the window method for FIR filter designing, recommended by the Standard, may be successfully used for obtaining compliant PMU filters.

Several fully compliant fixed-frequency low-pass FIR filters for the M class PMU Standard signal processing model [1, 2] have been proposed. The filters have been designed by the window method with Blackman, Hann or Rife-Vincent class I window, as either the flat-top windows, or optimal min-max filters. Successful application of flat-top windows for accurate estimation of the phasor frequency and its rate of change is an important contribution of this work. The proposed LP FIR filters are good candidates for inclusion in a future version of the Standard [1, 2] as fully compliant reference filters.

Acknowledgments

This work was supported by the Polish National Science Centre under decision DEC-2012/05/B/ST7/01218 and by the AGH University of Science and Technology contract no 11.11.230.018.

Appendix A

The *Discrete-Time Fourier Transform* (DTFT) of the filter $h_M[n]$ (10) is defined as:

$$H_M(e^{j\Omega}) = \sum_{n=-N}^N h_M[n]e^{-j\Omega n}, \quad \Omega = 2\pi \frac{f}{f_s}. \quad (\text{A.1})$$

The DTFT of $h_M[n]$ (10) is the superposition of $2M + 1$ scaled and shifted in the frequency spectra of a rectangular window ($h_0[n]=1$ for $|n| \leq N$, otherwise 0):

$$H_M(e^{j\Omega}) = \sum_{m=-M}^M a_M[m]H_0(e^{j(\Omega-m\Omega_{DFT})}), \quad \Omega_{DFT} = \frac{2\pi}{2N+1}, \quad (\text{A.2})$$

where:

$$H_0(e^{j\Omega}) = \frac{\sin(\Omega(2N+1)/2)}{\sin(\Omega/2)}. \quad (\text{A.3})$$

The bandwidth of $h_M[n]$ increases with increasing M . By selecting the filter coefficients $a_M[m]$ along with the filter order M and length $L = 2N + 1$ it is possible to influence the passband flatness, passband width, transition band width, and stopband attenuation of the filter spectrum (A.2).

Perfectly flat-top filters are obtained by putting the following constraints upon the filter frequency response:

1) DC gain:

$$H_M(e^{j0}) = L. \quad (\text{A.4})$$

2) $2R$ -order flatness at $\Omega=0$, i.e. zeroing its first $2R$ derivatives at $\Omega=0$:

$$\left. \frac{d^{2r}}{d^{2r}\Omega} H_M(e^{j\Omega}) \right|_{\Omega=0} = 0, \quad r = 1, 2, \dots, R. \quad (\text{A.5})$$

In (A.5) R denotes a parameter to be chosen, odd order derivatives of $H_M(e^{j\Omega})$ are neglected since they are always equal to zero for $\Omega=0$.

The conditions (A.4) and (A.5) may be expressed as [26]:

$$\sum_{m=0}^M a_M[m]C_N^r[m] = 0, \quad r = 0, 1, 2, \dots, R, \quad (\text{A.6})$$

where:

$$C_N^r[m] = \sum_{n=-N}^N n^{2r} \cos(m \frac{\pi}{N} n). \quad (\text{A.7})$$

Reducing discontinuity of the filter $h_M[n]$ (10) at $n = \pm N$ increases the sidelobe decaying speed. By zeroing $h_M[n]$ and its first Q derivatives over n at $n = N$ the following conditions for coefficients $h_M[m]$ can be derived for $q = 1, 2, 3, \dots, Q$ [29]:

$$h_M[N] = 0 \rightarrow \sum_{m=0}^M (-1)^m a_M[m] = 0, \quad (\text{A.8})$$

$$\left. \frac{d^{2q}}{d^{2q}n} h_M[n] \right|_{n=N} = 0 \rightarrow \sum_{m=0}^M (-1)^m m^{2q} a_M[m] = 0. \quad (\text{A.9})$$

In (A.9) only the even order derivatives are considered because all odd order derivatives are equal to 0 for $n = N$. For a rectangular filter the sidelobes decaying speed is 6 dB/OCT. Then, fulfilling $h_M[N] = 0$ (A.8) adds an extra 12 dB/OCT to this speed, and zeroing successive even order time derivatives of $h_M[n]$ for $n = N$ (A.9) adds another 12 dB/OCT (per each derivative).

The flat-top filter design procedure is based on solving a set of equations in the least mean square sense (LSQ). The equations are chosen from (A.6), (A.8), (A.9). When M coefficients $a_M[m]$ are to be found, only M constraints can be used. The following set of $M + 1 = (R+1)+1+Q$ equations is finally solved in a single step in the LSQ sense:

$$(R+1) \times (A.6) + (A.8) + Q \times (A.9). \quad (A.10)$$

The equation (A.8) is always used, thus the asymptotic rate of falloff of sidelobes is no slower than that for the Hann window, i.e. -18 dB per octave.

A Matlab program for computation of the flat-top filter coefficients $a_M[m]$ is presented in [26].

Appendix B

Implemented in Matlab function `phasor_estimation`, Program 1, estimates the instantaneous phase, amplitude, frequency, and rate of change of frequency of the signal x sampled with the frequency f_s for the system nominal frequency f_0 with an FIR filter having the impulse response h . An example of using this function is given in Program 2.

Program 1

```
function [pe, Xe, fe, ROCOFe] = phasor_estimation(x, h, f0, fs)
% x - time signal
% h - impulse response of estimating FIR filter
% f0 - nominal signal frequency
% fs - sampling frequency
% pe - estimated instantaneous phase in (rad)
% Xe - estimated instantaneous amplitude
% fe - estimated instantaneous frequency (Hz)
% ROCOFe - estimated Rate of Change of Frequency (Hz/s)
L = length(h);
N = (L-1)/2;
n = -N:N;
w0 = 2*pi*f0/fs;
h = 2*h(:) .* exp(j*w0*n(:)) / (L*mean(h));
y = conv(x, h);
pe = unwrap( angle(y));
Xe = abs(y);
fe = conv( pe, [1 0 -1]/2 )/(1/fs)/(2*pi); fe(1:1)=[];
ROCOFe = conv( fe, [1 0 -1]/2 )/(1/fs); ROCOFe(1:1)=[];
```

Program 2

```
clear all, close all, clc
%% Parameters
fs = 800; % sampling frequency in Hz
f0 = 50; % nominal frequency in Hz
Tmax = 10; % test signal length in s
t = [0:1/fs:Tmax-1/fs]; % time vector
%% Test signal
Xm = 1; % signal amplitude
if(1) % joint amplitude and phase modulation test
kx = 0.1; % the amplitude modulation factor
ka = 0.1; % the phase angle modulation factor
fm = 1; % modulation frequency in Hz
Xt = Xm*(1+kx*cos(2*pi*fm*t)); % instantaneous amplitude
Pt = ka*cos(2*pi*fm*t-pi); % instantaneous phase
d1Pt = f0-ka*fm*sin(2*pi*fm*t-pi); % frequency (1st phase derivative)
d2Pt = -ka*2*pi*fm.^2*cos(2*pi*fm*t-pi); % ROCOF (2nd phase derivative)
```

```

else % frequency ramp test
    framp = -5; % ramp starts at f0+framp Hz
    Xt = Xm*ones(size(t)); % instantaneous amplitude
    Pt = pi*t.^2+2*pi*framp*t; % instantaneous phase
    d1Pt = f0+t+framp; % frequency (1st phase derivative)
    d2Pt = ones(size(t)); % ROCOF (2nd phase derivative)
end
x = Xt.*cos(2*pi*f0*t+Pt); % test signal
%% Phasor estimation
M = 5; % Filter M=5, D0=2, DN=2, L=207 (Table I)
L = 207;
a5= [1.004854368932 2.007611297343 1.917918999420 ...
     1.451047039136 0.666862839032 0.130977870905];
N = (L-1)/2;
n = -N:N;
h = zeros(size(n));
for m=0:M
    h = h + a5(m+1)*cos(m*pi/N*n); % (10)
end
[Pte, Xte, fe, ROCOFe]=phasor_estimation(x, h, f0, fs);
%% Errors
t = t(N+1:end-N);
Pt = Pt(N+1:end-N);
Xt = Xt(N+1:end-N);
d1Pt = d1Pt(N+1:end-N);
d2Pt = d2Pt(N+1:end-N);
Pte = Pte(L:length(t)+L-1)-2*pi*f0*t;
Xte = Xte(L:length(t)+L-1);
fe = fe(L:length(t)+L-1);
ROCOFe = ROCOFe(L:length(t)+L-1);
Pt = unwrap( angle( exp(j*Pt) ) );
Pte = unwrap( angle( exp(j*Pte) ) );
err_phase = Pte-Pt;
err_ampl = Xte-Xt;
err_freq = fe-d1Pt;
err_ROCOF = ROCOFe-d2Pt;
figure,
    plot(t, err_phase, '-r', t, err_ampl, '-g', ...
         t, err_freq, '-b', t, err_ROCOF, '-k')
    legend('phase error (rad)', 'X error (.)', ...
          'f error (Hz)', 'ROCOF error (Hz/s)')
    xlabel('t (s)'), box on, grid on, axis tight

```

References

- [1] Synchrophasor Measurements for Power Systems, IEEE Standard C37.118.1, Dec. 2011.
- [2] Synchrophasor Measurements for Power Systems – Amendment 1: Modification of Selected Performance Requirements, IEEE Standard C37.118.1a, Apr. 2014.
- [3] Phadke, A.G., Thorp J.S. (2008). *Synchronized Phasor Measurements and Their Applications*. Springer.
- [4] Phadke, A.G., Thorp J.S. (2009). *Computer Relaying For Power Systems*. John Wiley and Sons.
- [5] Premerlani, W., Kasztenny, B., Adamiak, M. (2008). Development and implementation of a synchrophasor estimator capable of measurements under dynamic conditions. *IEEE Trans. Power Del.*, 23(1), 109–123.
- [6] Phadke, A., Kasztenny, B. (2009). Synchronized phasor and frequency measurement under transient conditions. *IEEE Trans. Power Del.*, 24(1), 89–95.
- [7] Macii, D., Petri, D., Zorat, A. (2012). Accuracy analysis and enhancement of DFT-based synchrophasor estimators in off-nominal conditions. *IEEE Trans. Instrum. Meas.*, 61(10), 2653–2664.

- [8] Belega, D., Petri, D. (2013). Accuracy analysis of the multicycle synchrophasor estimator provided by the interpolated DFT algorithm. *IEEE Trans. Instrum. Meas.*, 62(5), 942–953.
- [9] Petri, D., Fontanelli, D., Macii, D. (2014). A frequency-domain algorithm for dynamic synchrophasor and frequency estimation. *IEEE Trans. Instrum. Meas.*, 63(10), 2330–2340.
- [10] Barchi, G., Fontanelli, D., Macii, D., Petri, D. (2015). On the Accuracy of Phasor Angle Measurements in Power Networks. *IEEE Trans. Instrum. Meas.*, 64(5), 1129–1139.
- [11] Barchi, G., Macii, D., Petri, D. (2013). Synchrophasor estimators accuracy: A comparative analysis. *IEEE Trans. Instrum. Meas.*, 62(5), 963–973.
- [12] Barchi, G., Macii, D., Belega, D., Petri, D. (2013). Performance of synchrophasor estimators in transient conditions: A comparative analysis. *IEEE Trans. Instrum. Meas.*, 62(9), 2410–2418.
- [13] de la O Serna, J.A. (2007). Dynamic Phasor Estimates for Power System Oscillation. *IEEE Trans. on Instrum. Meas.*, 56(5), 1648–1657.
- [14] Platas-Garza, M. A., de la O Serna, J. A. (2010). Dynamic phasor and frequency estimates through maximally flat differentiators. *IEEE Trans. Instrum. Meas.*, 59(7), 1803–1811.
- [15] de la O Serna, J. A. (2015). Synchrophasor Measurement With Polynomial Phase-Locked-Loop Taylor–Fourier Filters. *IEEE Trans. on Instrum. Meas.*, 64(2), 328–337.
- [16] Belega, D., Fontanelli, D., Petri, D. (2015). Dynamic Phasor and Frequency Measurements by an Improved Taylor Weighted Least Squares Algorithm. *IEEE Trans. Instrum. Meas.*, 64(8), 2165–2178.
- [17] Belega, D., Macii, D., Petri, D. (2014). Fast synchrophasor estimation by means of frequency-domain and time-domain algorithms. *IEEE Trans. Instrum. Meas.*, 63(2), 388–401.
- [18] Roscoe, A.J., Dickerson, B., Martin, K.E. (2015). Filter Design Masks for C37.118.1a-Compliant Frequency-Tracking and Fixed-Filter M-Class Phasor Measurement Units. *IEEE Trans. on Instrum. Meas.*, 64(8), 2096–2107.
- [19] Roscoe, A.J., Abdulhadi, I.F., Burt, G.M. (2013). P and M class phasor measurement unit algorithms using adaptive cascaded filters. *IEEE Trans. Power Del.*, 28(3), 1447–1459.
- [20] Roscoe, A.J. (2013). Exploring the relative performance of frequency-tracking and fixed-filter phasor measurement unit algorithms under C37.118 test procedures, the effects of interharmonics, and initial attempts at Mering P-class response with M-class filtering. *IEEE Trans. Instrum. Meas.*, 62(8), 2140–2153.
- [21] Kamwa, I., Samantaray, S.R., Joos, G. (2014). Wide Frequency Range Adaptive Phasor and Frequency PMU Algorithms. *IEEE Trans. Smart Grid.*, 5(2), 569–579.
- [22] Kamwa, I., Samantaray, S., Joos, G. (2013). Compliance analysis of PMU algorithms and devices for wide-area stabilizing control of large power systems. *IEEE Trans. Power Syst.*, 28(2), 1766–1778.
- [23] Castello, P., Liu, J., Muscas, C., Pegoraro, P.A., Ponci, F., Monti, A. (2014). A fast and accurate PMU algorithm for P+M class measurement of synchrophasor and frequency. *IEEE Trans. Instrum. Meas.*, 63(12), 2837–2845.
- [24] Martin, K.E. (2015). Synchrophasor measurements under the IEEE standard C37.118.1-2011 with amendment C37.118.1a. *IEEE Trans. Power Del.*, 30(3), 1514–1522.
- [25] Oppenheim, A.V., Schaffer, R.W., Buck, J.R. (1999). *Discrete-Time Signal Processing, 2nd Edition*. Prentice-Hall.
- [26] Duda, K., Zielinski, T.P., Barcentewicz, Sz. (2016). Perfectly Flat-Top and Equiripple Flat-Top Cosine Windows. *IEEE Trans. on Instrum. Meas.*, 65(7), 1558–1567.
- [27] Signal Processing Toolbox 6 User’s Guide, The Mathworks Inc., Natick, MA, USA, Sep. 2010.
- [28] Harris, F.J. (1978). On the use of windows for harmonic analysis with the discrete Fourier transform. *Proc. IEEE*, 66, 51–83.
- [29] Nuttall, A.H. (1981). Some Windows with Very Good Sidelobe Behavior. *IEEE Trans. On Acoustics, Speech, And Signal Processing*, ASSP-29(1), 84–91.